

## Accelerated Publications

### A Substrate in Pieces: Allosteric Activation of Glycerol 3-Phosphate Dehydrogenase (NAD<sup>+</sup>) by Phosphite Dianion<sup>†</sup>

Wing-Yin Tsang, Tina L. Amyes, and John P. Richard\*

*Department of Chemistry, University at Buffalo, State University of New York, Buffalo, New York 14260-3000*

*Received January 30, 2008; Revised Manuscript Received March 5, 2008*

**ABSTRACT:** The ratio of the second-order rate constants for reduction of dihydroxyacetone phosphate (DHAP) and of the neutral truncated substrate glycolaldehyde (GLY) by glycerol 3-phosphate dehydrogenase (NAD<sup>+</sup>, GPDH) saturated with NADH is  $(1.0 \times 10^6 \text{ M}^{-1} \text{ s}^{-1}) / (8.7 \times 10^{-3} \text{ M}^{-1} \text{ s}^{-1}) = 1.1 \times 10^8$ , which was used to calculate an intrinsic phosphate binding energy of at least 11.0 kcal/mol. Phosphite dianion binds very weakly to GPDH ( $K_d > 0.1 \text{ M}$ ), but the bound dianion strongly activates GLY toward enzyme-catalyzed reduction by NADH. Thus, the large intrinsic phosphite binding energy is expressed *only* at the transition state for the GPDH-catalyzed reaction. The ratio of rate constants for the phosphite-activated and the unactivated GPDH-catalyzed reduction of GLY by NADH is  $(4300 \text{ M}^{-2} \text{ s}^{-1}) / (8.7 \times 10^{-3} \text{ M}^{-1} \text{ s}^{-1}) = 5 \times 10^5 \text{ M}^{-1}$ , which was used to calculate an intrinsic phosphite binding energy of  $-7.7$  kcal/mol for the association of phosphite dianion with the transition state complex for the GPDH-catalyzed reduction of GLY. Phosphite dianion has now been shown to activate bound substrates for enzyme-catalyzed proton transfer, decarboxylation, hydride transfer, and phosphoryl transfer reactions. Structural data provide strong evidence that enzymic activation by the binding of phosphite dianion occurs at a modular active site featuring (1) a binding pocket complementary to the reactive substrate fragment which contains all the active site residues needed to catalyze the reaction of the substrate piece or of the whole substrate and (2) a phosphate/phosphite dianion binding pocket that is completed by the movement of flexible protein loop(s) to surround the nonreacting oxydianion. We propose that loop motion and associated protein conformational changes that accompany the binding of phosphite dianion and/or phosphodianion substrates lead to encapsulation of the substrate and/or its pieces in the protein interior, and to placement of the active site residues in positions where they provide optimal stabilization of the transition state for the catalyzed reaction.

Enzymes are protein catalysts that effect rate accelerations much larger than those observed for small molecule catalysts. The larger rate accelerations for enzymes are a consequence of the greater binding affinities of enzymes for their reaction transition states (*I*). Enzyme catalysis is so efficient that the release of products would be intolerably slow if they were

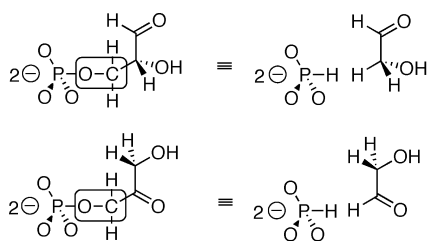
to bind with the same affinity as the transition state. For example, the ca. 30 kcal/mol transition state intrinsic binding energy estimated for the enzymatic decarboxylation of orotidine 5'-monophosphate (OMP)<sup>1</sup> catalyzed by orotidine

<sup>†</sup> This work was supported by Grant GM39754 from the National Institutes of Health.

\* To whom correspondence should be addressed. Telephone: (716) 645-6800, ext. 2194. Fax: (716) 645-6963. E-mail: jrichard@chem.buffalo.edu.

<sup>1</sup> Abbreviations: OMP, orotidine 5'-monophosphate; OMPDC, orotidine 5'-monophosphate decarboxylase; GAP, (R)-glyceraldehyde 3-phosphate; TIM, triosephosphate isomerase; GPDH, glycerol 3-phosphate dehydrogenase (NAD<sup>+</sup>); DHAP, dihydroxyacetone phosphate; NADH, nicotinamide adenine dinucleotide, reduced form; α-GP, L-glycerol 3-phosphate; GLY, glycolaldehyde; BSA, bovine serum albumin; DTT, D,L-dithiothreitol; TEA, triethanolamine; NMR, nuclear magnetic resonance.

Scheme 1



**Holistic Substrate**      **Two-Part Substrate**

5'-monophosphate decarboxylase (OMPDC) (2) is even larger than the 20 kcal/mol binding energy associated with the effectively irreversible binding of biotin to avidin (3). Consequently, to avoid this free energy "trap", enzymes generally bind their substrates and/or products much more weakly than the reaction transition state.

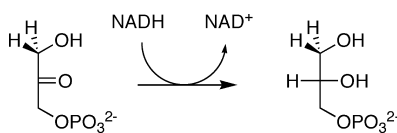
It has been proposed that enzymes often produce large rate accelerations through the utilization of binding interactions between the protein and nonreacting portions of the substrate for transition state stabilization (4, 5). However, the mechanism(s) by which enzyme catalysts selectively "turn on" these binding interactions at the transition state for their catalyzed reactions is not generally known, and this question is often omitted from discussions of the origin of the rate acceleration for enzyme catalysts.

The binding energy of the remote nonreacting phosphodianion groups of OMP and (*R*)-glyceraldehyde 3-phosphate (GAP) has been shown to provide a ca. 12 kcal/mol stabilization of the transition states for OMPDC-catalyzed decarboxylation (6) and proton transfer catalyzed by triose-phosphate isomerase (TIM) (7), respectively. Moreover, the small substrate "piece" phosphite dianion provides strong allosteric-like activation of OMPDC-catalyzed decarboxylation (6) and TIM-catalyzed deprotonation (8) of a second truncated substrate piece from which the phosphodianion group has been excised. The latter results show that a substantial fraction of the "intrinsic phosphate binding energy" is expressed as transition state stabilization even in the absence of a covalent connection between the substrate pieces. Phosphite dianion binds weakly to both TIM ( $K_d = 38$  mM) (8) and OMPDC ( $K_d = 140$  mM) (6) so that the large intrinsic phosphite binding energy is expressed only at the respective transition states for these enzyme-catalyzed reactions.

X-ray crystallographic analyses suggest that both TIM and OMPDC utilize the binding energy of the substrate phosphodianion group to drive the thermodynamically unfavorable closure of a mobile protein loop(s) to cover the bound phosphodianion (9–12). We have proposed (8) that this loop closure sequesters the substrate from bulk solvent and results in formation of a local microenvironment in which there is optimal stabilization of the transition state for the enzymatic reaction (13, 14).

We examine here whether the functional equivalence of GAP and the "two-part substrate" [glycolaldehyde + phosphite] (Scheme 1) for proton transfer catalyzed by TIM might also be observed for other types of enzymatic reactions. Glycerol 3-phosphate dehydrogenase (NAD<sup>+</sup>-linked, EC 1.1.1.8, GPDH) is used in the assay for TIM-catalyzed isomerization of GAP to couple formation of the product

Scheme 2



dihydroxyacetone phosphate (DHAP) to its reduction by NADH to give L-glycerol 3-phosphate [ $\alpha$ -GP (Scheme 2)] (15). We report here that GPDH also catalyzes the very slow reduction of the neutral minimal substrate glycolaldehyde (GLY) by NADH and that the separate binding of the second substrate piece phosphite dianion strongly activates GPDH for catalysis of the reduction of GLY by NADH. We conclude that the substrate pieces [glycolaldehyde + phosphite] are able to effectively substitute for the whole substrate GAP or DHAP in enzyme-catalyzed proton transfer and hydride transfer reactions, respectively.

## MATERIALS AND METHODS

**Materials.** Glycerol 3-phosphate dehydrogenase (lyophilized powder, 75 units/mg) from rabbit muscle was purchased from USB Corp. Bovine serum albumin, fraction V (BSA), was from Roche. Dihydroxyacetone phosphate (lithium salt), NADH (disodium salt), glycolaldehyde dimer, triethanolamine hydrochloride, D,L-dithiothreitol (DTT), and sodium deuterioxide (40 wt %, 99.9% D) were from Sigma-Aldrich. Deuterium oxide (99.9% D) was from Cambridge Isotope Laboratories. Sodium phosphate (dibasic) was from Fluka, and sodium phosphite (dibasic, pentahydrate) was from Riedel-de Haen (Fluka). Water was from a Milli-Q Academic purification system. All other chemicals were reagent grade or better and were used without further purification.

**Preparation of Solutions.** The solution pH was determined as described previously (8). Stock solutions of NADH were prepared by dissolving NADH (disodium salt) in water and were stored at 4 °C. The concentration of NADH was determined spectrophotometrically at 340 nm using an  $\epsilon$  of 6220 M<sup>-1</sup> cm<sup>-1</sup>. Stock solutions of DHAP were prepared on the day of the experiment by dissolving the lithium salt in water and adjusting the pH to 7.5 using 1 M NaOH and were stored on ice. The concentration of DHAP was determined spectrophotometrically at 340 nm as the concentration of NADH oxidized in a reaction catalyzed by GPDH. GPDH (2 or 20 mg/mL) in 20 mM triethanolamine (TEA) buffer (pH 7.5, 32% free base) was dialyzed exhaustively against the same buffer at 5 °C. The concentration of GPDH was determined from the absorbance at 280 nm using an  $A$  of 5.15 for a 1% solution of GPDH (16) and a subunit molecular mass of 37500 Da. Stock solutions of glycolaldehyde (100 mM monomer) were prepared by dissolving glycolaldehyde dimer in water and storing the solution for at least 3 days at room temperature to allow for breakdown of the dimer to the monomer (8). An apparent  $pK_a$  of 6.38 for phosphite monoanion at 25 °C and an  $I$  of 0.12 (NaCl) was determined as the pH of a 30 mM solution of the sodium salt at a 1:1 monoanion:dianion ratio.

**Enzyme Assays.** Dilutions of the dialyzed stock solutions of 2 mg/mL enzyme (used for assays of GPDH-catalyzed reduction of DHAP) and 20 mg/mL enzyme (used for assays of GPDH-catalyzed reduction of GLY) were made in 20 mM TEA (pH 7.5, 32% free base) containing 10 mM DTT.

All enzyme assays were conducted at 25 °C and an *I* of 0.12 (NaCl) in a volume of 1 mL. Initial velocities of oxidation of NADH ( $\leq 5\%$  reaction) were calculated from the changes in absorbance at 340 nm using a  $\Delta\epsilon$  of 6220 M<sup>-1</sup> cm<sup>-1</sup>. The standard assay mixture for GPDH activity contained 100 mM TEA (pH 7.5), 1.2 mM DHAP, 0.20 mM NADH, 0.1 mg/mL BSA, 50  $\mu$ M DTT, and ca. 1 nM GPDH at an *I* of 0.12 (NaCl). Reactions were initiated by making a 200-fold dilution of the diluted stock enzyme containing 10 mM DTT into the reaction mixture. The same procedure was used to determine the velocity of GPDH-catalyzed reduction over a range of initial concentrations of DHAP, except that the buffer was 20 mM TEA (pH 7.5).

Assay mixtures for the GPDH-catalyzed reduction of GLY in the absence of phosphite contained 10 mM TEA (pH 7.5), 20 mM GLY (total), 0.20 mM NADH, and up to ca. 0.2 mM GPDH at an *I* of 0.12 (NaCl). Assay mixtures for the GPDH-catalyzed reduction of GLY in the presence of phosphite contained 10 mM TEA (pH 7.5), 2–60 mM GLY (total), 0.20 mM NADH, up to 32 mM phosphite dianion, and 0.6  $\mu$ M GPDH at an *I* of 0.12 (NaCl).

<sup>1</sup>H NMR Analyses. <sup>1</sup>H NMR spectra at 500 MHz were recorded in D<sub>2</sub>O at 25 °C using a Varian Unity Inova 500 spectrometer as described previously (8). The product of the GPDH-catalyzed reduction of GLY by NADH in a reaction mixture containing 10 mM TEA (pD 8.0), 31 mM sodium phosphite (93% dianion), 5 mM GLY (total), and 7 mM NADH in D<sub>2</sub>O was identified by <sup>1</sup>H NMR spectroscopy. The reaction was initiated by the addition of 380  $\mu$ L of GPDH in buffered D<sub>2</sub>O (pD 8.0, 20 mM TEA) to give a total volume of 1 mL and a final enzyme concentration of 11  $\mu$ M. A second <sup>1</sup>H NMR spectrum, recorded after reaction for 12 h, showed the disappearance of ca. 80% of the starting GLY and the appearance of a singlet at 3.53 ppm, which was shown to be due to the methylene protons of a corresponding amount of ethylene glycol by the addition of an authentic standard.

The fraction of GLY present in the free carbonyl form in H<sub>2</sub>O buffered by 10 mM TEA (pH 7.5) at 25 °C and an *I* of 0.12 (NaCl) ( $1 - f_{\text{hyd}}$ ) was determined by <sup>1</sup>H NMR spectroscopy using a coaxial inner tube containing D<sub>2</sub>O and suppression of the water peak. A value for  $1 - f_{\text{hyd}}$  of  $0.06 \pm 0.003$  was obtained by comparison of the integrated areas of the signals due to the C2 protons of the free carbonyl and hydrated forms of GLY, which is the same as a value for  $1 - f_{\text{hyd}}$  of 0.06 determined previously for the hydration of GLY in D<sub>2</sub>O at pD 7.0, 25 °C, and an *I* of 0.10 (8).

## RESULTS

Initial velocities,  $v_i$ , of the reduction of DHAP by NADH catalyzed by GPDH at pH 7.5 (10 mM TEA), 25 °C, and an *I* of 0.12 (NaCl) were determined by monitoring the decrease in absorbance at 340 nm. Figure 1A shows the dependence of  $v_i$  (M s<sup>-1</sup>) on the total concentration of DHAP in the presence of 0.10 mM ( $\blacktriangle$ ) or 0.20 mM ( $\bullet$ ) NADH and 1.1 nM GPDH. The solid line shows the fit of the data to the Michaelis–Menten equation with a ( $K_m$ )<sub>app</sub> value of 0.24 mM and a  $V_{\text{max}}$  value of  $1.42 \times 10^{-7}$  M s<sup>-1</sup>. The latter was used to calculate a  $k_{\text{cat}}$  value of 130 s<sup>-1</sup>, and a  $K_m$  value of 0.13 mM for the reactive free carbonyl form of DHAP was calculated using a value for  $1 - f_{\text{hyd}}$  of 0.55 for the fraction

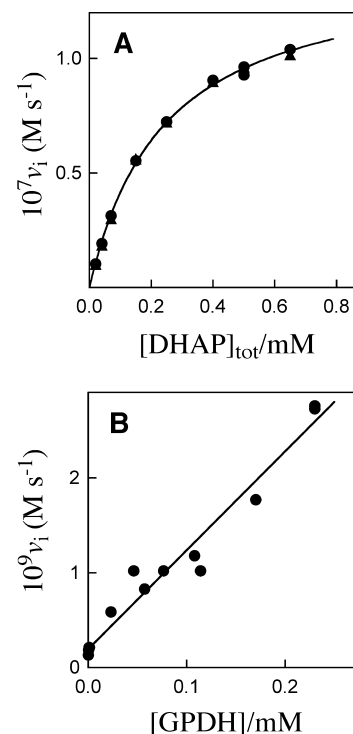


FIGURE 1: (A) Dependence of the initial velocity,  $v_i$ , of the reduction of DHAP by NADH catalyzed by GPDH (1.1 nM) on the total concentration of DHAP in the presence of 0.10 mM ( $\blacktriangle$ ) or 0.20 mM ( $\bullet$ ) NADH at pH 7.5, 25 °C, and an *I* of 0.12 (NaCl). (B) Dependence of the initial velocity,  $v_i$ , of the reduction of GLY (20 mM total, 1.2 mM free carbonyl form) by NADH (0.20 mM) on the concentration of GPDH at pH 7.5, 25 °C, and an *I* of 0.12 (NaCl).

Table 1: Kinetic Parameters for Reduction of Dihydroxyacetone Phosphate and Glycolaldehyde Catalyzed by GPDH and for Activation by Phosphite Dianion<sup>a</sup>

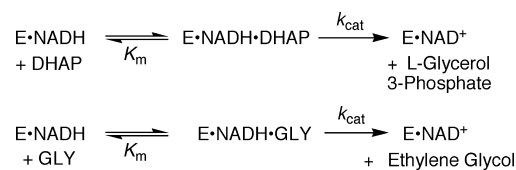
substrate	activator	$K_m^b$ (mM)	$k_{\text{cat}}$ (s <sup>-1</sup> )	$k_{\text{cat}}/K_m$ (M <sup>-1</sup> s <sup>-1</sup> )	$K_d^c$ (M)	$k_{\text{cat}}/K_{ia}K_b$ (M <sup>-2</sup> s <sup>-1</sup> )
DHAP <sup>d</sup>		0.13	130	$1.0 \times 10^6$		
GLY <sup>e</sup>				$(8.7 \pm 0.5) \times 10^{-3}$		
GLY <sup>f</sup>	HPO <sub>3</sub> <sup>2-</sup>	$8 \pm 1$			>0.1	$4300 \pm 700$

<sup>a</sup> At pH 7.5 (10 mM TEA buffer), 25 °C, and an *I* of 0.12 (NaCl).

<sup>b</sup> Values of  $K_m$  refer to the free carbonyl form of DHAP or GLY.

<sup>c</sup> Dissociation constant for the phosphite dianion activator. <sup>d</sup> Kinetic parameters determined from data shown in Figure 1A. <sup>e</sup> Kinetic parameters determined from data shown in Figure 1B. <sup>f</sup> Kinetic parameters determined from data shown in Figure 2.

### Scheme 3



of DHAP present in the free carbonyl form (Scheme 3) (17). These data (Table 1) are in agreement with the published kinetic parameters for GPDH (18).

There is a ca. 50% decrease in the activity of GPDH (60  $\mu$ M) during an 8 h incubation at pH 7.5 (10 mM TEA) in the presence of 1.2 mM GLY (free carbonyl form, 20 mM total GLY) and 0.20 mM NADH at 25 °C and an *I* of 0.12 (NaCl). Figure 1B shows the dependence of the initial velocity  $v_i$  (M s<sup>-1</sup>) of the reduction of GLY under these

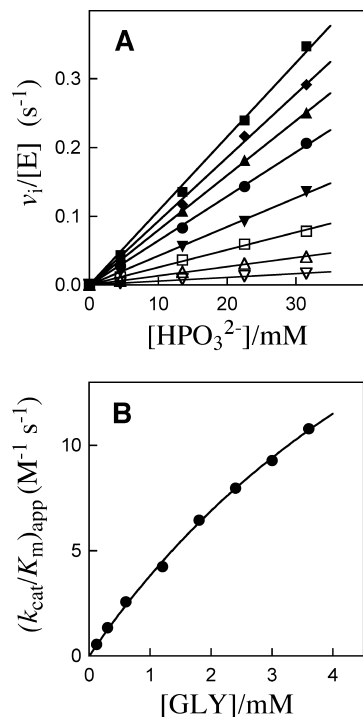
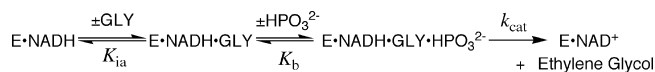


FIGURE 2: (A) Dependence of  $v_i/[E]$  for the reduction of GLY by NADH (0.20 mM) catalyzed by GPDH (0.6  $\mu$ M) on the concentration of exogenous phosphite dianion at pH 7.5, 25 °C, and an  $I$  of 0.12 (NaCl). Concentrations of GLY (free carbonyl form) were ( $\nabla$ ) 0.12, ( $\triangle$ ) 0.30, ( $\square$ ) 0.60, ( $\blacktriangledown$ ) 1.2, ( $\bullet$ ) 1.8, ( $\blacktriangle$ ) 2.4, ( $\blacklozenge$ ) 3.0, and ( $\blacksquare$ ) 3.6 mM. (B) Dependence of the apparent second-order rate constant  $(k_{cat}/K_m)_{app}$  for the phosphite-activated GPDH-catalyzed reduction of GLY by NADH (0.20 mM) on the concentration of GLY at pH 7.5, 25 °C, and an  $I$  of 0.12 (NaCl), calculated as the slopes of the correlations in panel A.

conditions on the concentration of GPDH, determined from the decrease in absorbance at 340 nm (0.01–0.02 OD unit) observed at early reaction times ( $\leq 60$  min) where the velocity is constant. The loss of activity of GPDH during this time, determined by a periodic standard assay, was  $<10\%$ . The slope of the correlation in Figure 1B gives the apparent first-order rate constant for the enzymatic reduction of GLY as  $(1.04 \pm 0.06) \times 10^{-5} \text{ s}^{-1}$ .<sup>2</sup> The second-order rate constant for enzyme-catalyzed reduction of GLY (Scheme 3) can then be calculated with the relationship  $(k_{cat}/K_m)_{GLY} = (1.04 \times 10^{-5} \text{ s}^{-1})/[GLY] = (8.7 \pm 0.5) \times 10^{-3} \text{ M}^{-1} \text{ s}^{-1}$ , where  $[GLY]$  (1.2 mM) is the concentration of GLY present in the reactive free carbonyl form.

Figure 2A shows that there is a linear dependence of  $v_i/[E]$  (s<sup>-1</sup>) for the reduction of various concentrations of GLY by NADH (0.20 mM) catalyzed by GPDH (0.6  $\mu$ M) on the concentration of exogenous phosphite dianion at pH 7.5 (10 mM TEA), 25 °C, and an  $I$  of 0.12 (NaCl). The addition of phosphite dianion results in very large increases in  $v_i$  for these GPDH-catalyzed reactions, and <sup>1</sup>H NMR analysis confirmed that the product of the reduction of GLY by NADH in the presence of phosphite dianion is ethylene glycol (Scheme 4). The failure to observe curvature in the correlations shown in Figure 2A requires that phosphite dianion bind very weakly to GPDH so that the concentrations of both the ternary complex  $E \cdot NADH \cdot HPO_3^{2-}$  and the

Scheme 4



quaternary complex  $E \cdot NADH \cdot GLY \cdot HPO_3^{2-}$  are each much smaller than the total concentration of GPDH over the range of  $HPO_3^{2-}$  concentrations examined. The data were therefore fit to eq 1, derived for a reaction mechanism in which there is no significant formation of the  $E \cdot NADH \cdot HPO_3^{2-}$  complex (Scheme 4). The linear correlations in Figure 2A show that  $[HPO_3^{2-}] \ll K_b$ , and the slopes of these correlations correspond to apparent second-order rate constants  $(k_{cat}/K_m)_{app}$  (M<sup>-1</sup> s<sup>-1</sup>) for the phosphite-activated GPDH-catalyzed reduction of GLY by NADH (eq 2).

$$v_i/[E] = \frac{k_{cat}[GLY][HPO_3^{2-}]}{[GLY][HPO_3^{2-}] + K_b[GLY] + K_{ia}K_b} \quad (1)$$

$$(k_{cat}/K_m)_{app} = \frac{(k_{cat}/K_b)[GLY]}{K_{ia} + [GLY]} \quad (2)$$

Figure 2B shows the dependence of  $(k_{cat}/K_m)_{app}$ , determined as the slopes of the correlations in Figure 2A, on the concentration of the free carbonyl form of glycolaldehyde. The solid line shows the fit of the data to eq 2, which gave a  $K_{ia}$  value of  $8 \pm 1$  mM for binding of GLY and a  $k_{cat}/K_b$  value of  $35 \pm 4 \text{ M}^{-1} \text{ s}^{-1}$  (Scheme 4). The slope of the correlation in Figure 2B at low concentrations of GLY corresponds to the third-order rate constant  $k_{cat}/K_{ia}K_b$  ( $4300 \pm 700 \text{ M}^{-2} \text{ s}^{-1}$ ) for the phosphite-activated GPDH-catalyzed reduction of GLY by NADH. The kinetic parameters determined in this work are summarized in Table 1.

The velocity of the GPDH-catalyzed reduction of DHAP by NADH (0.20 mM) at  $[DHAP] = K_m$ , pH 7.5 (10 mM TEA), 25 °C, and an  $I$  of 0.12 (NaCl) was found to decrease by 15% upon the inclusion of 33 mM phosphite dianion, while 35 mM sulfate dianion causes a somewhat larger 36% decrease in the velocity under the same reaction conditions. These small changes in velocity show that both phosphite and sulfate dianions bind only weakly to GPDH. The evaluation of  $K_i$  binding constants for these dianions is complicated by uncertainties about whether there are also specific salt effects on the kinetic parameters for the GPDH-catalyzed reaction.

## DISCUSSION

The cofactor  $NAD^+$  is a competitive product inhibitor of the GPDH-catalyzed reduction of DHAP when NADH is the varied substrate but a noncompetitive inhibitor when DHAP is the varied substrate (19). The sugar L-glycerol 3-phosphate is a noncompetitive product inhibitor of the GPDH-catalyzed reduction of DHAP when either NADH or DHAP is the varied substrate, but the inhibition with respect to NADH changes to uncompetitive when the reaction is carried out in the presence of saturating concentrations of DHAP (19). These results provide strong evidence for an ordered mechanism, with NADH binding first followed by DHAP (18, 19). A similar ordered mechanism is assumed to hold for reduction of the two-part substrate [glycolaldehyde + phosphite] by NADH, with the cofactor binding first, followed by binding of the substrate pieces GLY and

<sup>2</sup> Quoted errors are standard deviations obtained from the linear or nonlinear least-squares fit of the data. Errors in calculated quantities were computed using standard equations for the propagation of error.



Table 2: Comparison of the Intrinsic Phosphate Binding Energies and the Observed and Total Intrinsic Phosphite Binding Energies for Enzyme-Catalyzed Decarboxylation, Proton Transfer, and Hydride Transfer Reactions<sup>a</sup>

Enzymatic Reaction	$(k_{\text{cat}}/K_m)_{\text{SPi}}^b$ $\text{M}^{-1} \text{s}^{-1}$	$(k_{\text{cat}}/K_m)_s^c$ $\text{M}^{-1} \text{s}^{-1}$	Intrinsic Phosphate Binding Energy <sup>d</sup>	$(k_{\text{cat}}/K_m)_s/K_d^e$ $\text{M}^{-2} \text{s}^{-1}$	Observed and Total Intrinsic Phosphite Binding Energy <sup>f</sup>
OMP $\xrightarrow[\text{CO}_2]{\text{OMPDc}}$ UMP Decarboxylation <sup>g</sup>	$9.4 \times 10^6$	0.021	-11.8 kcal/mol	12,000	-1.2 kcal/mol -7.8 kcal/mol
GAP $\xrightarrow{\text{TIM}}$ DHAP Proton Transfer <sup>h</sup>	$2.4 \times 10^8$	0.26	-12.2 kcal/mol	4900	-1.9 kcal/mol -5.8 kcal/mol
DHAP $\xrightarrow[\text{E} \cdot \text{NADH} \rightarrow \text{E} \cdot \text{NAD}^+]{\text{GPDH}}$ $\alpha$ -GP Hydride Transfer <sup>i</sup>	$1.0 \times 10^6$	0.0087	$\leq -11.0$ kcal/mol	4300	$> -1.4$ kcal/mol -7.7 kcal/mol

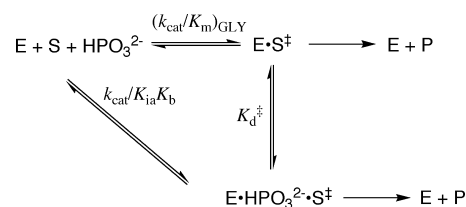
<sup>a</sup> Binding energies are defined to be negative when the binding is thermodynamically favorable. <sup>b</sup> Second-order rate constant for turnover of the whole phosphorylated natural substrate by the free enzyme. <sup>c</sup> Second-order rate constant for turnover of the neutral truncated substrate lacking a phosphodianion group by the free enzyme. <sup>d</sup> Calculated from the rate constant ratio  $(k_{\text{cat}}/K_m)_{\text{SPi}}/(k_{\text{cat}}/K_m)_s$ . <sup>e</sup> Third-order rate constant for enzyme-catalyzed reaction of the neutral truncated substrate activated by phosphite dianion. <sup>f</sup> Energy for binding of phosphite dianion to the free enzyme (top number) and to the transition state complex  $\text{E} \cdot \text{S}^\ddagger$  (bottom number). <sup>g</sup> Data from ref 6. <sup>h</sup> Data from ref 8. <sup>i</sup> Data from this work.

phosphite dianion (Scheme 4). A Michaelis constant of 6.3  $\mu\text{M}$  for NADH has been reported for the GPDH-catalyzed reduction of DHAP at pH 7.8 (19). The essentially identical dependence of the initial velocity of GPDH-catalyzed reduction on DHAP concentration in the presence of 0.10 or 0.20 mM NADH at pH 7.5 (Figure 1A) shows that under our reaction conditions GPDH is completely saturated by the lower concentration of NADH. Studies of the reduction of GLY and of the phosphite-activated reduction of GLY catalyzed by GPDH were carried out in the presence of 0.20 mM NADH so that the concentration of the  $\text{E} \cdot \text{NADH}$  complex is given by the total concentration of enzyme.

**Reaction of the Substrate in Pieces.** The Michaelis–Menten plots for the reduction of DHAP catalyzed by GPDH at 0.10 or 0.20 mM NADH and pH 7.5 (Figure 1A) give a  $K_m$  of 0.13 mM for the free carbonyl form of DHAP and a  $k_{\text{cat}}/K_m$  of  $1.0 \times 10^6 \text{ M}^{-1} \text{s}^{-1}$  as the second-order rate constant for reduction of DHAP by the  $\text{E} \cdot \text{NADH}$  complex. By comparison, a value for  $(k_{\text{cat}}/K_m)_{\text{GLY}}$  of  $(8.7 \pm 0.5) \times 10^{-3} \text{ M}^{-1} \text{s}^{-1}$  was determined for reduction of the truncated substrate GLY by the  $\text{E} \cdot \text{NADH}$  complex (Figure 1B). We conclude that the substrate phosphodianion group activates DHAP toward GPDH-catalyzed reduction by NADH by at least  $10^8$ -fold. This likely underestimates the phosphodianion group activation because the aldehyde group of GLY is intrinsically more reactive toward a nucleophilic hydride donor than the keto group of DHAP. These data show that the enzymatic transition state for hydride transfer from enzyme-bound NADH to DHAP is stabilized by at least 11 kcal/mol by interactions between GPDH and the nonreacting phosphodianion group of the substrate (Table 2).

The GPDH-catalyzed reduction of GLY by NADH is strongly activated by the second substrate piece phosphite dianion. Figure 2A shows that plots of  $v_i/[\text{E}]$  ( $\text{s}^{-1}$ ) for reduction of various concentrations of GLY by NADH (0.20 mM) at pH 7.5 [ $I = 0.12$  (NaCl)] against  $\text{HPO}_3^{2-}$  concentration are linear up to at least 33 mM phosphite dianion. The same concentration of phosphite dianion results in only a 15% reduction in the initial velocity of GPDH-catalyzed

Scheme 5



reduction of DHAP by NADH when  $[\text{DHAP}] = K_m$ . We conclude that phosphite dianion binds only weakly to GPDH ( $K_d > 0.1 \text{ M}$  for dissociation of the  $\text{E} \cdot \text{HPO}_3^{2-}$  complex) but that this dianion provides an impressive activation of reduction of the second substrate piece GLY by NADH catalyzed by GPDH.

The slopes of the linear correlations in Figure 2A correspond to apparent second-order rate constants  $(k_{\text{cat}}/K_m)_{\text{app}}$  for the phosphite-activated reduction of GLY catalyzed by the  $\text{E} \cdot \text{NADH}$  complex. Figure 2B shows that these apparent second-order rate constants appear to approach a limiting value for reactions at high concentrations of the hydride acceptor GLY. The fit of the data in Figure 2B to eq 2 (derived for Scheme 4) gave a  $k_{\text{cat}}/K_{\text{ia}}K_b$  of  $4300 \pm 700 \text{ M}^{-2} \text{s}^{-1}$  as the third-order rate constant for reaction of the two substrate pieces GLY and  $\text{HPO}_3^{2-}$  with the  $\text{E} \cdot \text{NADH}$  complex to form ethylene glycol and  $\text{NAD}^+$ . Scheme 5 shows that the intrinsic affinity of  $\text{HPO}_3^{2-}$  for the GPDH–transition state complex  $\text{E} \cdot \text{S}^\ddagger$ , defined as a  $K_d^\ddagger$  of 2  $\mu\text{M}$  for the  $\text{E} \cdot \text{HPO}_3^{2-} \cdot \text{S}^\ddagger$  complex, can be calculated as the ratio of the second-order rate constant for unactivated enzyme-catalyzed reduction of GLY,  $(k_{\text{cat}}/K_m)_{\text{GLY}}$ , and the third-order rate constant for reaction of the substrate pieces,  $k_{\text{cat}}/K_{\text{ia}}K_b$ , according to eq 3.

$$K_d^\ddagger = \frac{(k_{\text{cat}}/K_m)_{\text{GLY}}}{k_{\text{cat}}/K_{\text{ia}}K_b} = \frac{0.0087 \text{ M}^{-1} \text{s}^{-1}}{4300 \text{ M}^{-2} \text{s}^{-1}} = 2.0 \mu\text{M} \quad (3)$$

The observation of linear plots in Figure 2A for the phosphite-activated enzyme-catalyzed reduction of GLY by NADH shows that there is no detectable accumulation of

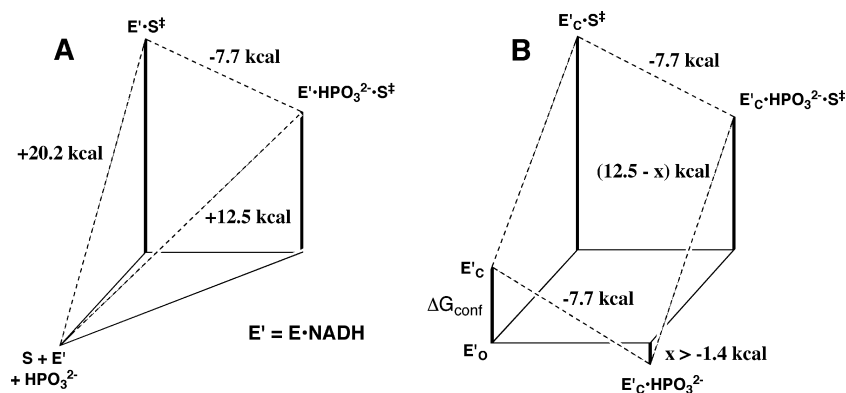


FIGURE 3: (A) Free energy diagram for turnover of the truncated neutral substrate GLY (S) by the binary GPDH•NADH complex (E') and for the same reaction activated by the binding of exogenous phosphite dianion ( $\text{HPO}_3^{2-}$ ). Activation free energies were calculated using the Eyring equation at 298 K. The weakly bound Michaelis complex  $\text{E}'\cdot\text{HPO}_3^{2-}$  is not shown, because the stability of this complex is not defined by our experiments. (B) Free energy diagram illustrating our proposed model for activation of E' toward reduction of GLY by the binding of  $\text{HPO}_3^{2-}$ . Binding energies are defined to be negative when the binding is thermodynamically favorable. The difference between the total intrinsic phosphite binding energy of  $-7.7$  kcal/mol and the observed binding energy  $x$  of greater than  $-1.4$  kcal/mol for binding of  $\text{HPO}_3^{2-}$  to the inactive open enzyme  $\text{E}'_O$  to give the active closed enzyme  $\text{E}'_C\cdot\text{HPO}_3^{2-}$  is the binding energy that is used to convert  $\text{E}'_O$  to  $\text{E}'_C$ . The observed  $\Delta G^\ddagger$  value of 20.2 kcal/mol for turnover of GLY (panel A) has been partitioned into the  $\Delta G^\ddagger$  for reduction of GLY by  $\text{E}'_C$  and the  $\Delta G_{\text{conf}}$  for the unfavorable conformational change that converts  $\text{E}'_O$  to  $\text{E}'_C$ .

the  $\text{E}\cdot\text{HPO}_3^{2-}$  complex at  $\leq 33$  mM  $\text{HPO}_3^{2-}$ . Therefore, the binding of phosphite dianion to the free enzyme is not shown in Scheme 5, because the stability of the  $\text{E}\cdot\text{HPO}_3^{2-}$  complex relative to the free enzyme is not defined by our experiments.

Scheme 5 is represented graphically in Figure 3A. The large activation barrier of ca. 20 kcal/mol for the direct bimolecular reduction of the truncated neutral substrate GLY by the  $\text{E}\cdot\text{NADH}$  complex was calculated from the second-order rate constant ( $k_{\text{cat}}/K_m$ )<sub>GLY</sub> [ $(8.7 \pm 0.5) \times 10^{-3} \text{ M}^{-1} \text{ s}^{-1}$  (Table 1)] using the Eyring equation at 298 K. The smaller activation barrier for the phosphite-activated reduction of GLY was calculated from the third-order rate constant  $k_{\text{cat}}/K_{\text{ia}}K_b$  [ $4300 \pm 700 \text{ M}^{-2} \text{ s}^{-1}$  (Table 1)]. The 7.7 kcal/mol larger activation barrier for reduction of GLY catalyzed by the  $\text{E}\cdot\text{NADH}$  complex compared to that for its phosphite-activated reduction is equal to the stabilization associated with the binding of phosphite dianion to the transition state complex  $\text{E}\cdot\text{S}^\ddagger$  to give the complex  $\text{E}\cdot\text{HPO}_3^{2-}\cdot\text{S}^\ddagger$ , for which  $K_d^\ddagger = 2 \mu\text{M}$ .

**Mobile Loops and Catalysis.** X-ray crystallographic analysis of GPDH from *Leishmania mexicana* shows that the GPDH•NAD<sup>+</sup>•DHAP ternary complex adopts a “closed” form relative to the free, unliganded, enzyme (20). It has been proposed that the formation of stabilizing interactions between the phosphodianion group of bound DHAP and amino acid side chains at mobile protein elements provides the major driving force for closure of the protein pocket (20, 21). This is analogous to the closure of flexible loops around the phosphodianion group of bound intermediate analogues at TIM (11, 12, 22) and at OMPDC (9, 23). In these cases, loop closure and the formation of interactions with the substrate phosphodianion group were proposed to activate the substrates GAP/DHAP and OMP for the respective enzyme-catalyzed proton transfer (8) and decarboxylation (6) reactions.

Figure 3B is a free energy diagram that illustrates one physical mechanism for activation of GPDH toward reduction of glyceraldehyde by the binding of exogenous phosphite dianion. In this model, we propose that a large fraction of the intrinsic binding energy of  $-7.7$  kcal/mol for the

phosphite dianion activator is *utilized* to drive a thermodynamically unfavorable change in the conformation of the enzyme from an inactive open form,  $\text{E}'_O$  ( $\text{E}' = \text{E}\cdot\text{NADH}$ ), to an active loop-closed form,  $\text{E}'_C$ . The *observed* binding of phosphite dianion to the free enzyme is therefore only weakly favorable, with a binding energy  $x > -1.4$  kcal/mol, because the total intrinsic phosphite binding energy is largely offset by the unfavorable free energy associated with the conformational changes that accompany binding of this substrate piece ( $\Delta G_{\text{conf}} = 7.7 + x$  kcal/mol). We also propose that a large fraction of the intrinsic binding energy of the transition state for reduction of the neutral substrate piece GLY,  $\text{S}^\ddagger$ , is utilized to drive the same loop closure and conformational change. The full intrinsic binding energy of  $\text{HPO}_3^{2-}$  or of the transition state  $\text{S}^\ddagger$  is then observed only when these species bind to the loop-closed forms of GPDH,  $\text{E}'_C\cdot\text{S}^\ddagger$  or  $\text{E}'_C\cdot\text{HPO}_3^{2-}$ , respectively.

We propose that the large selectivity of phosphite dianion for binding to  $\text{E}'_C$  rather than to  $\text{E}'_O$  results from the formation of stabilizing interactions between this oxydianion and amino acid side chains at mobile protein elements that move to form the loop-closed protein, and that very similar interactions are formed between the protein and the phosphodianion group of the whole substrate DHAP. The proposed large selectivity of the transition state for binding to  $\text{E}'_C$  would require that loop closure result in formation of a local environment that is more favorable for transformation of the bound substrate to the transition state for hydride transfer than that at the open enzyme  $\text{E}'_O$ . We are able only to speculate about these changes, because the imperatives for enzymatic catalysis of hydride transfer from NADH have not been well defined.

Loop closure that sequesters the substrate from aqueous solvent at a nonpolar active site should have the effect of increasing the extent of transition state stabilization available from hydrogen bonding and ion pairing interactions between the protein and the bound ligand (24). For example, the magnitude of the stabilizing electrostatic interactions between enzymic hydrogen bond donors and the partial negative charge that develops at the carbonyl oxygen in

the transition state for hydride transfer from NADH to glycolaldehyde will increase with a decrease in the effective dielectric constant of the reaction medium (25). It is possible that loop closure when substrate binds to GPDH results in a decrease in the separation between the hydride donor and the hydride acceptor at the Michaelis complex. This would narrow the width of the potential energy barrier that separates reactants and products, and it could favor quantum mechanical tunneling through this barrier (26). Finally, loop closure may have the effect of “ordering” the catalytic groups in the active site to provide optimal transition state stabilization by minimizing the entropic barrier to the enzyme-catalyzed reaction (13).

**How Do Enzymes Work?** Glucose 1-phosphate and glucose 6-phosphate are rapidly phosphorylated by the phosphoserine of phosphoglucomutase to form glucose 1,6-diphosphate. In 1976, B. Ray showed that enzyme-catalyzed phosphorylation of xylose by this enzyme is very slow, but that this phosphoryl transfer reaction is strongly activated by binding of the second substrate piece phosphite dianion (27). It has taken 30 years to generalize these results from studies of an enzyme-catalyzed phosphoryl group transfer reaction to enzyme-catalyzed proton transfer (8), hydride transfer (this work), and decarboxylation reactions (6). Our work on three different enzymes that catalyze mechanistically diverse heterolytic reactions has shown that these catalysts have achieved strikingly similar efficiencies in their utilization of the intrinsic binding energy of the substrate phosphodianion group in catalysis (Table 2).

(1) OMPDC, TIM, and GPDH exhibit similar  $10^8$ – $10^9$ -fold lower activities for catalysis of the reaction of a truncated substrate that lacks a phosphodianion group, ( $k_{\text{cat}}/K_m$ )<sub>s</sub>, than for catalysis of the reaction of the whole substrate, ( $k_{\text{cat}}/K_m$ )<sub>SP<sub>i</sub></sub>. These results suggest that an important outcome of the biological phosphorylation of sugars is to provide enzyme catalysts with an electrostatic handle from which they may obtain ca. 12 kcal/mol of intrinsic binding energy.

(2) Each of these very slow enzyme-catalyzed reactions of the appropriate truncated neutral substrate piece is strongly activated by the separate binding of exogenous phosphite dianion.

(3) In each case, the second-order rate constant ( $k_{\text{cat}}/K_m$ )<sub>SP<sub>i</sub></sub> for reaction of the “whole” substrate is larger than the third-order rate constant for the phosphite-activated reaction of the truncated substrate piece [4300–12000 M<sup>-2</sup> s<sup>-1</sup> (see Table 2)]. The difference between the second-order rate constant for reaction of the whole substrate and the third-order rate constant for reaction of the pieces reflects the large entropic advantage of the unimolecular reaction of the whole substrate, compared with the bimolecular reaction of the pieces (28).

(4) The individual substrate pieces exhibit low affinities for the formation of productive Michaelis complexes. However, tethering the two pieces gives a whole substrate that exhibits an enhanced binding affinity due to the chelate effect (28).

(5) In each case, binding of the substrate phosphodianion group drives the movement of mobile protein loop(s) to close the active site and cover the phosphate group, which effectively buries the reactive substrate fragment in the

protein interior. The binding of phosphite dianion presumably drives a similar conformational change (8).

Apparently, these diverse proteins have adopted a common modular design to effect very efficient enzymatic catalysis from utilization of the intrinsic binding energy of the nonreacting phosphate fragment of the substrate. This design features (a) an active site that recognizes the reactive substrate fragment and which contains all of the catalytic amino acid side chains needed to execute the chemistry of catalyzed reaction and (b) a neighboring site for a second nonreactive substrate piece (for example, phosphite dianion), which is completed by the movement of flexible protein loops over this piece. This loop movement encapsulates the reactive substrate piece within the protein where the local dielectric constant is smaller than that of water, where the catalytic side chains are positioned to provide optimal transition state stabilization, and where other electrostatic factors may also favor transition state stabilization.

In recent years, there have been, at best, small incremental advances in the de novo rational design of synthetic small molecule catalysts or of high molecular mass protein or nucleic acid catalysts. We suggest that the recognition and understanding of this modular design element in enzymes that have evolved to effectively utilize “intrinsic phosphate binding energy” may guide the efforts of chemical biologists interested in the de novo design of proteins with enzymelike catalytic activities.

## REFERENCES

- Pauling, L. (1948) The nature of forces between large molecules of biological interest. *Nature* 161, 707–709.
- Radzicka, A., and Wolfenden, R. (1995) A proficient enzyme. *Science* 267, 90–93.
- Green, N. M. (1966) Thermodynamics of the binding of biotin and some analogues by avidin. *Biochem. J.* 101, 774–780.
- Jencks, W. P. (1975) Binding Energy, Specificity and Enzymic Catalysis: The Circe Effect. *Adv. Enzymol. Relat. Areas Mol. Biol.* 43, 219–410.
- Jencks, W. P. (1987) Economics of enzyme catalysis. *Cold Spring Harbor Symp. Quant. Biol.* 52, 65–73.
- Amyes, T. L., Richard, J. P., and Tait, J. J. (2005) Activation of orotidine 5'-monophosphate decarboxylase by phosphite dianion: The whole substrate is the sum of two parts. *J. Am. Chem. Soc.* 127, 15708–15709.
- Amyes, T. L., O'Donoghue, A. C., and Richard, J. P. (2001) Contribution of phosphate intrinsic binding energy to the enzymatic rate acceleration for triosephosphate isomerase. *J. Am. Chem. Soc.* 123, 11325–11326.
- Amyes, T. L., and Richard, J. P. (2007) Enzymatic catalysis of proton transfer at carbon: Activation of triosephosphate isomerase by phosphite dianion. *Biochemistry* 46, 5841–5854.
- Miller, B. G., Hassell, A. M., Wolfenden, R., Milburn, M. V., and Short, S. A. (2000) Anatomy of a proficient enzyme: The structure of orotidine 5'-monophosphate decarboxylase in the presence and absence of a potential transition state analog. *Proc. Natl. Acad. Sci. U.S.A.* 97, 2011–2016.
- Miller, B. G., Snider, M. J., Short, S. A., and Wolfenden, R. (2000) Contribution of enzyme-phosphoribosyl contacts to catalysis by orotidine 5'-phosphate decarboxylase. *Biochemistry* 39, 8113–8118.
- Lolis, E., and Petsko, G. A. (1990) Crystallographic analysis of the complex between triosephosphate isomerase and 2-phosphoglycolate at 2.5-Å resolution: Implications for catalysis. *Biochemistry* 29, 6619–6625.
- Davenport, R. C., Bash, P. A., Seaton, B. A., Karplus, M., Petsko, G. A., and Ringe, D. (1991) Structure of the triosephosphate isomerase-phosphoglycolohydroxamate complex: An analog of the intermediate on the reaction pathway. *Biochemistry* 30, 5821–5826.

13. Cannon, W. R., and Benkovic, S. J. (1998) Solvation, reorganization energy, and biological catalysis. *J. Biol. Chem.* **273**, 26257–26260.
14. Warshel, A. (1998) Electrostatic Origin of the Catalytic Power of Enzymes and the Role of Preorganized Active Sites. *J. Biol. Chem.* **273**, 27035–27038.
15. Plaut, B., and Knowles, J. R. (1972) pH-Dependence of the triose phosphate isomerase reaction. *Biochem. J.* **129**, 311–320.
16. Bentley, P., Dickinson, F. M., and Jones, I. G. (1973) Purification and properties of rabbit muscle L-glycerol 3-phosphate dehydrogenase. *Biochem. J.* **135**, 853–859.
17. Reynolds, S. J., Yates, D. W., and Pogson, C. I. (1971) Dihydroxyacetone phosphate. Its structure and reactivity with  $\alpha$ -glycerolphosphate dehydrogenase, aldolase and triose phosphate isomerase and some possible metabolic implications. *Biochem. J.* **122**, 285–297.
18. Bentley, P., and Dickinson, F. M. (1974) A study of the kinetics and mechanism of rabbit muscle L-glycerol 3-phosphate dehydrogenase. *Biochem. J.* **143**, 19–27.
19. Black, W. J. (1966) Kinetic studies on the mechanism of cytoplasmic L- $\alpha$ -glycerophosphate dehydrogenase of rabbit skeletal muscle. *Can. J. Biochem. Phys.* **44**, 1301–1317.
20. Suresh, S., Turley, S., Oppendoes, F. R., Michels, P. A. M., and Hol, W. G. H. (2000) A potential target enzyme for trypanocidal drugs revealed by the crystal structure of NAD-dependent glycerol-3-phosphate dehydrogenase from *Leishmania mexicana*. *Structure* **8**, 541–552.
21. Ou, X., Ji, C., Han, X., Zhao, X., Li, X., Mao, Y., Wong, L.-L., Bartlam, M., and Rao, Z. (2006) Crystal structures of human glycerol 3-phosphate dehydrogenase 1 (GPD1). *J. Mol. Biol.* **357**, 858–869.
22. Zhang, Z., Sugio, S., Komives, E. A., Liu, K. D., Knowles, J. R., Petsko, G. A., and Ringe, D. (1994) Crystal structure of recombinant chicken triosephosphate isomerase-phosphoglycolohydroxamate complex at 1.8-Å resolution. *Biochemistry* **33**, 2830–2837.
23. Begley, T. P., Appleby, T. C., and Ealick, S. E. (2000) The structural basis for the remarkable catalytic proficiency of orotidine 5'-monophosphate decarboxylase. *Curr. Opin. Struct. Biol.* **10**, 711–718.
24. Richard, J. P., and Amyes, T. L. (2004) On the importance of being zwitterionic: Enzymic catalysis of decarboxylation and deprotonation of cationic carbon. *Bioorg. Chem.* **32**, 354–366.
25. Hine, J. (1975) *Structural effects on equilibria in organic chemistry*, John Wiley & Sons, New York.
26. Kohen, A., and Klinman, J. P. (1998) Enzyme catalysis: Beyond classical paradigms. *Acc. Chem. Res.* **31**, 397–404.
27. Ray, W. J., Jr., and Long, J. W. (1976) Thermodynamics and mechanism of the  $\text{PO}_3$  transfer process in the phosphoglucomutase reaction. *Biochemistry* **15**, 3993–4006.
28. Jencks, W. P. (1981) On the attribution and additivity of binding energies. *Proc. Natl. Acad. Sci. U.S.A.* **78**, 4046–4050.

BI8001743